



# Effective Cross Section of Cold Formed Steel Column Under Axial Compression

P. Manikandan<sup>1</sup> · T. Pradeep<sup>2</sup>

Received: 23 February 2017 / Accepted: 4 February 2018  
© The Institution of Engineers (India) 2018

**Abstract** The compressive resistance of cold-formed steel (CFS) section may be governed by local, distortional or overall buckling and any apparent interaction between these modes. A new inventive stiffened CFS section is elected in this study, selected cross sections geometries and lengths are chosen such that all the types of buckling modes are met with. Buckling plot is plotted using linear elastic buckling analysis software (CUFSM). Using the test results obtained in the literature, the developed finite element model is calibrated and furthers a total of 126 parametric study is conducted such as a consequence of dimensions and the length of the cross section, thickness and yield stress. The FEA included relevant material and geometric imperfections. All the columns are analyzed under pin end conditions with axial compression. The analysis results demonstrate that the DSM equations generally assess the strength of stiffened section conservatively. Modifications to the DSM equations are recommended to evaluate the strength of stiffened section more precisely.

**Keywords** Buckling · Cold-formed steel · Compression member · Direct strength method · Finite-element analysis

## Introduction

Generally, basic types of buckling in thin-walled steel column is local, distortion and overall. Based on the geometry of the cross section, slenderness ratio, end boundary condition and loading condition any one of the buckling modes or interaction of buckling modes may occur. For the structural applications in the construction industry, open and closed cold-formed steel sections are familiar. Moreover, open or closed profile, the width of the element increases local buckling effortlessly occurred and drastically affects the behaviour of the member. In such circumstances, intermediate or edge stiffener improves the behaviour of the member, related to this many of the researchers successfully completed the research and many articles available at global forum. To minimize the local buckling of the flat elements V, U and corrugated shape intermediate stiffeners are commonly used in the construction industry. Though many of the research had been fulfilled in the behaviour of cold-formed section with V, U and corrugated shape intermediate stiffener, but the results are speckled in the behaviour of cold-formed section with corrugated shape intermediate stiffener. Consequently, in this study, a new innovative stiffened CFS is considered and meticulous parametric study is carried out.

## Review of Literature

Research into the buckling behaviour of cold-formed steel section has concerned significant awareness in recent years. The design specifications for an edge and intermediate stiffened elements was first to propose by the researchers [1]. Similarly, local and distortional buckling interaction of thin-walled sections was foremost to report by the

✉ P. Manikandan  
lp\_mani@yahoo.com

<sup>1</sup> Department of Civil Engineering, Centre for SONA Structural Engineering Research, Sona College of Technology, Salem, Tamil Nadu, India

<sup>2</sup> Department of Civil Engineering, K.S.Rangasamy College of Technology, Namakkal, Tamil Nadu, India

researchers [2], similar studies were conducted by the literatures [3–5]. Recently, local/distortional/global interaction research carried out by the researchers [6–10]. Likewise, distortional buckling behaviour was conducted by the researchers [11–13]. Stub column tests of thin-walled complex section with intermediate stiffeners were discussed by the author [14], in continuation of this by author have again numerically studied by the author [15], using FEA, effect of intermediate stiffener on the flange and web, geometric imperfection, slenderness ratio and end boundary conditions on the distortional buckling strength of the complex thin walled section. They also evaluate the effectiveness of DSM equations and also provide the modifications of the same for the complex thin walled section. The author [16] evaluates the suitability of AISC, AISI and DSM equation for locally slender columns and gave the suitable recommendation for the design methods. Failure analysis of composite lipped channel columns under axial compression discussed by the author [17].

To conquer numerous difficulties in design, such as complex cross section shapes and time consuming, modification on the calculation on the basis of the Direct Strength Method (DSM) by the author [18] on design of cold formed steel column against distortional failure, by the author [19] on design of storage rack column, by the author [20] discussed on of web-stiffened lipped channel columns with distortional and local mode interaction, by the author [21] evaluate on lipped channel column with local distortional interaction. Only, very limited studies are reported in the investigation on thin-walled complex section with intermediate stiffeners (corrugated) and results are scattered. This paper further investigates the buckling behaviour of thin-walled complex section with intermediate stiffeners (corrugated).

The aspire of this paper is to present the FEA results and structural behaviour of new innovative stiffened CFS section in axial compression with pin ended boundary conditions. Buckling plots are plotted using finite strip analysis program CUFSM. Numerical simulations are conducted using ANSYS software. Initially, a finite element model is developed and results are validated with the test results available from the literature reported by [22]. The results are confirmed by the test results. Initially, the validated FE models are used for stiffening evaluation of flat element towards stiffened element is carried out and developed a new innovative stiffened CFS section. Finally, a total of 126 FEA parametric studies is carried out to investigate the effect of the size of the cross sectional element, thickness and length of new innovative stiffened CFS section. All the test results are compared with the Direct Strength Method (DSM) for cold-formed steel structures. The analysis results demonstrate that the DSM equations generally assess the strength of stiffened section conservatively.

Modifications to the DSM equations are recommended to evaluate the strength of stiffened section more precisely.

## Details of Finite-Element Model

ANSYS version 12 is used to produce the strength data by nonlinear FEA of the pin-ended cold formed steel stiffened (CFS-SC) columns. Initially, to standardize the FE model, a few existing test results of compression members failing after dissimilar buckling modes are analysed. Afterward, the FEA is used to thoroughly study the full series of parameters that may influence the strength and behaviour of stiffened section (SC) sections. SC members are modelled using four noded shell 181 element along the centre line thickness of the plate element of the cross-sections. To minimize/avoid stress concentration at ends because of the application of load and/or boundary conditions, structural 3D mass element with high-bending stiffness in the plane of the shell are provided, linking all the nodes along the edges of a shell element at the two ends of the member (Fig. 1). The similar mass elements are used to connect every node at the two ends of the member to the master nodes at the centroid of the end cross section. The axial load and end-boundary conditions are strained at the master node at the two end. Figure 1 shows the distinctive FE mesh used in the analysis, finalized subsequent to a convergence study. Two consequent methods are used to perform the analysis of the columns. The earliest step is a linear buckling analysis is done using the geometry of the perfect member, to identify the probable buckling modes. Subsequent to this, non-linear static eigen buckling

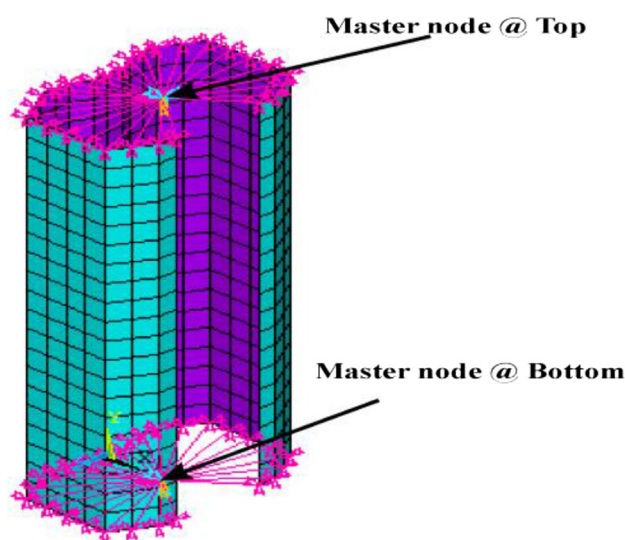
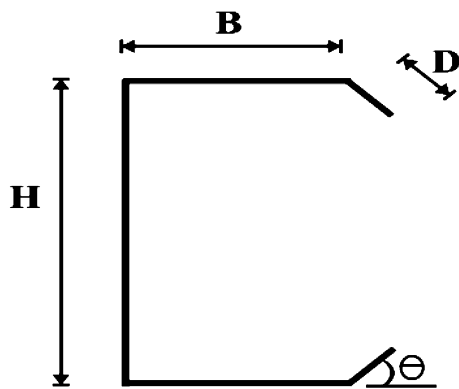


Fig. 1 Details of FEA model

**Table 1** Comparison of finite element and experimental results of channel column with inclined edge stiffeners tested by Zhang et al. [22]

Specimen ID	Section Dimensions (mm)				$\theta$ (degree)	$P_{EXP}$	$P_{ANSYS}$	% Diff
	H	B	D	L				
0500A45	160.16	78.54	18.74	499.4	44.8	266.16	276.64	- 3.94
2000A135	160.08	78.79	18.96	1991.2	134.4	231.26	233.77	- 1.09
1250A135	159.65	79.19	18.64	1248.9	133.1	280.66	281.03	- 0.13
500A90	159.97	80.64	19.96	498.9	89.1	298.97	294.886	1.37
500A135	159.03	80.44	18.09	499	131.8	293.25	304.392	- 3.80
700A90	160.35	81.55	19.45	699.7	89.9	295.25	272.864	7.58
Mean								- 0.001
SD								4.254



**Fig. 2** Cross section and symbols used [22]

analysis is performed on the identical mode. Considering both the material and geometric nonlinearities. The utmost amplitude of imperfections of 0.25 and 1.0 times the thickness of the elements [23, 24], related to the first local and distortional buckling modes from the eigenvalue buckling analysis, in that order, are applied in the nonlinear analysis model. In order to account for the elastic-perfectly plastic properties, a bilinear stress-strain curve is used with a tangent modulus of 2000 N/mm<sup>2</sup>.

### Verification of FE Model

For the calibration study, comparison of the ultimate load as obtained from FEA, corresponding to the 6 series of test results, chosen from the literature [22], is offered in Table 1, along with the values from the tests. Specimen is labeled such that the length, type of loading and angle of edge stiffener can be identified from the label. For an example “0500A45”, The first term defined the length of the member in millimeter (500 mm), the second term defined the type of lading (A- axial load) and the last term define the angle of inclination of edge stiffener in degrees. From the literature [22] it is observed that, specimens were tested both axial and eccentric loading conditions. In this study all the parametric analysis focused on the axial loading only. Hence, verification of FE model, totally 6 models was selected from the literature [22]. The selected cross section profile with nomenclature and corresponding dimensions obtained from the literature [22] are shows in Fig. 2 and Table 2 respectively. The comparison is good (Fig. 3), with the maximum difference in the ultimate load [ $P_{EXP}/P_{ANSYS} - 1$ ]  $\times$  100] being 7.8%. The Mean and the Standard deviation (SD) of the fraction dissimilarity of all 6 results are 0.001 and 4.254 respectively. This validated the satisfactoriness of FEA to generate data on  $P_{ul}$ . By means of FEA, a large volume of data on  $P_{ul}$  is generated

**Table 2** Cross section dimension and load capacities

S. no	Specimen ID	Section dimension (mm)					Cross-sectional area (Sq.m)	Ultimate strength (kN)	Failure modes
		A	B	C	D	H			
1	USC	95				160	560	23.29	LB
2	SC	-	-	70	25		560	45.29	LB + DB
3	SC-I	-	15	55	25		560	56.14	LB + DB
4	SC-II	-	15	55	25		560	114.41	DB
5	SC-III	15	15	40	25		560	116.15	DB

LB local buckling, DB distortional buckling

**Fig. 3** Verification of FEA model 0500A45 [22]

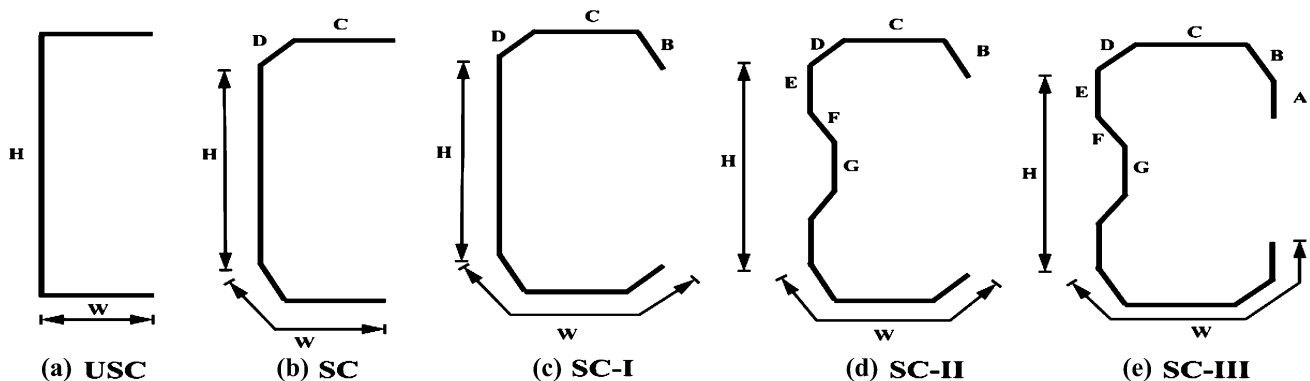
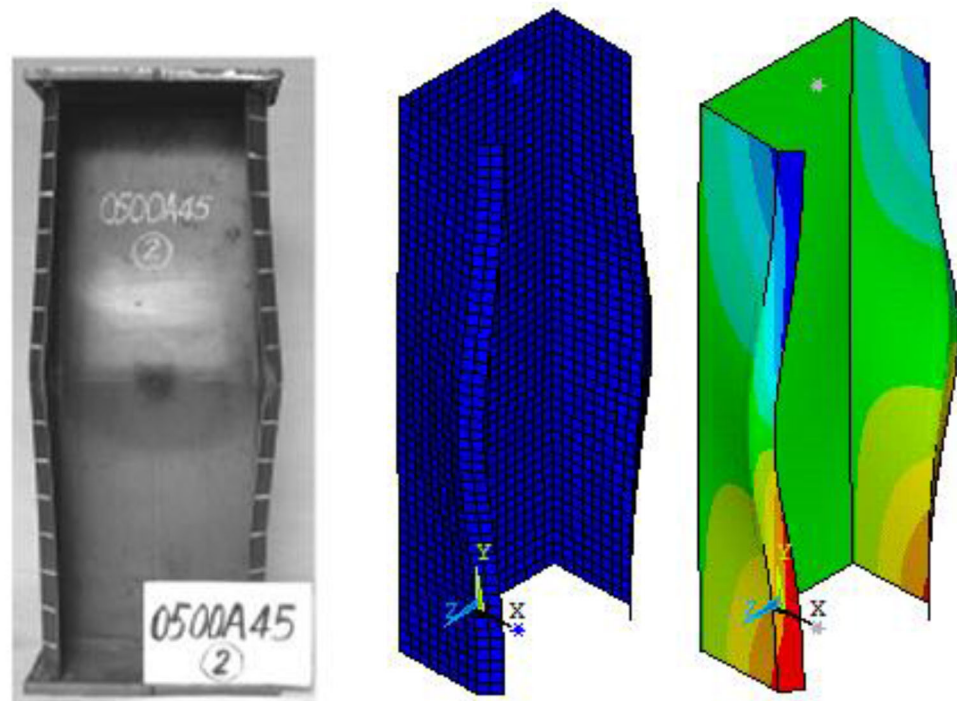


**Fig. 4** Section geometries

by methodically varying significant parameters. The particulars are presented in the succeeding section.

The intention of the present research is to estimate the ultimate strength and study the behaviour of thin-walled columns having the equal cross-sectional area with different cross sectional profile as shown in Fig. 4. Table 2 and Fig. 5 show the ultimate load and buckling behaviour of the specimens respectively. Specimens USC, SC, SC-I, SC-II and SC-III have the same equal cross sectional area, in which specimens USC is failed by local buckling, specimens SC and SC-I are failed by combined local and distortional buckling and their ultimate strengths are 23.29, 45.29 and 56.14 kN respectively. But specimens SC-II and SC-III are failed by distortional buckling and their ultimate strengths are 114.41 and 116.15 kN respectively. The

ultimate strength of the SC-II and SC-III series columns are higher than the all other columns (equal cross sectional area). From this study, it is observed that the SC series column exhibits higher capacity than unstiffened columns.

## Parametric Study

### Labeling

The specimens are tagging such that the type of column, variables and nominal length of the element is articulated by the label. For example, the label “SC-E1-10” defines the following specimen:

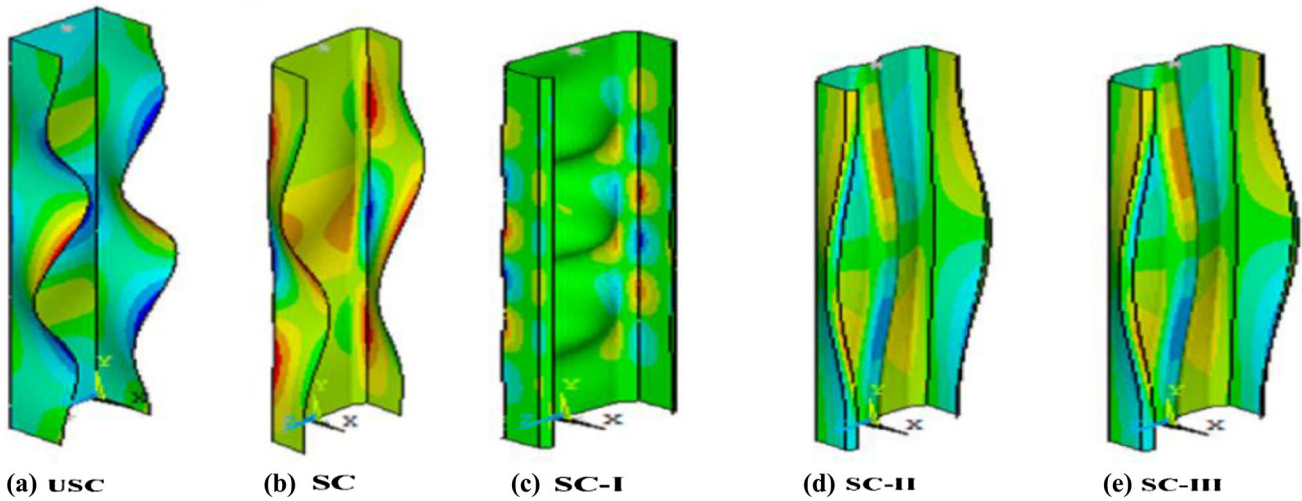


Fig. 5 Failure modes of all the specimens

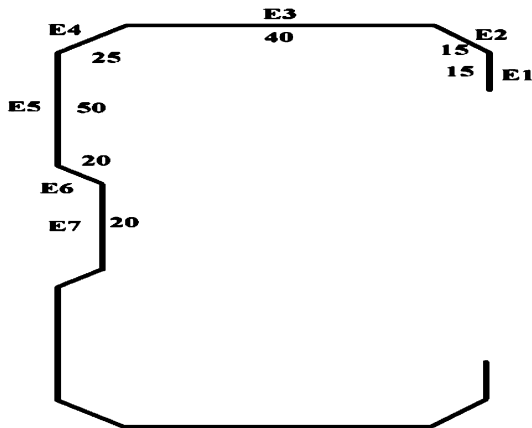


Fig. 6 Mean cross section geometries

1. The first two letters designate that the specimen is a stub column section (alternative IC-intermediate column and LC- long column).
2. The middle letter “E1” designate that the information of the element.
3. The final numerical values “10” designate that the size of the element in millimetre.

### Selection of Cross section

From this study, it is observed that the SC-III series column (Fig. 6) exhibits higher capacity and improve their behaviour than all other columns. Hence, a new innovative stiffened CFS section (SC-III series) is preferred for the parametric study. If section geometry deformation is allowed, then local and distortional buckling may occur. A small finite strip buckling analysis of mean section geometries (Fig. 5) is accomplished using CUFSM software as illustrated in Fig. 7. The local, interaction between

local and distortional, distortional and flexural buckling occurred has a minimum length of 100, 500, 1000 and 2000 mm respectively. Hence, in this study, a detailed investigation on all the length are carried out and details are offered in the consequent sections.

### Parameter Ranges

Finite element analysis on 126 pin-ended columns are carried out, using the validated FEM as described previously. The detailed parametric study is carried out for the extensive range of cross section dimensions such as size of the lip (E1), the width of the flange (E3), the depth of the web (E5), size of intermediate stiffener (E7), thickness of the section ( $t$ ) and yield stress of steel ( $f_y$ ) with three dissimilar column lengths. The list of ranges of various parameters and basic values for each parameter is presented in Table 3. The simulation studies are carried out by varying one variable at a time and keeping the other constant at the basic values of mean cross section geometries as illustrated in Fig. 6.

### Effect of Thickness Variation

In this parametric study, all the columns have a length of 1000 mm while keeping all other parameters are constant of mean cross section geometries as illustrated in Fig. 5 with three yield stresses (270,350 and 550 N/mm<sup>2</sup>). For an example, the effect of thickness variation ( $t$ ) for yield stress of 270 N/mm<sup>2</sup> is demonstrated in Fig. 8a for seven sectional thicknesses (0.60, 0.80, 1.20, 1.60, 2.00, 3.00 and 4.00 mm). Similarly, results are obtained for all the yield stress variations and results are tabulated in Table 4. It is observed that for a particular yield stress, ultimate load of the section increases with an increase in the thickness of

Fig. 7 Buckling plots

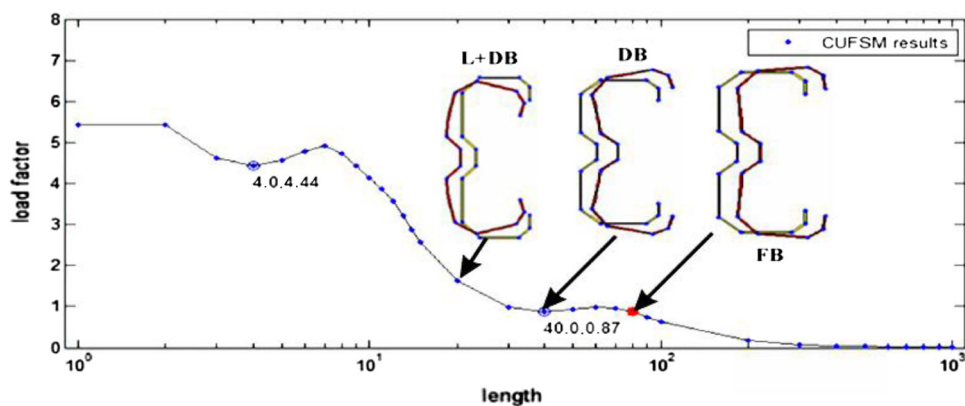


Table 3 List of variable parameters and its ranges

Variables	Range (mm)		Basic value
	Min	Max	
Column length (L)	500	2000	1000
Size of lip (E1)	10	70	15
Flange width (E3)	30	100	40
Web depth (E5)	30	80	50
Intermediate web stiffener (E7)	10	60	25
Thickness (t)	0.6	4.0	1.6
Yield Stress ( $f_y$ )	270	550	270

the section and stiffness of the section is increased by increasing the thickness of the section.

### Effect of Yield Variation

In this study, all the columns have a length of 1000 mm while keeping all other parameters are constant of mean cross section geometries as illustrated in Fig. 5 with three yield stresses (270,350 and 550 N/mm<sup>2</sup>) and seven sectional thicknesses (0.60, 0.80, 1.20, 1.60, 2.00, 3.00 and 4.00 mm). For an example, the effect of yield stress variation (270,350 and 550 N/mm<sup>2</sup>) is demonstrated in Fig. 8b for sectional thicknesses of 1.6 mm. Similarly, results are obtained for all the thickness variations and results are tabulated in Table 4. It is observed that for a particular thickness, ultimate load of the section increases with an increase in the yield stress of the section and stiffness of the section is remain constant by increasing the yield stress of the section (Table 5).

### Effect of Variation of Size of Lip

Figure 8c demonstrates the relationship between the size of lip (E1) and the ultimate load of the column for different lengths (500,1000 and 2000 mm) and size of lip varied

from 10 to 70 mm with increment of 10 mm while keeping all other factors same of mean cross section geometries for each finite element analysis. From the Fig. 7c, it can be observed that load carrying capacities of the section increases with the increase in the lip size and reduced by the increasing the lip size. The torsional rigidity at the compression flange to lip junction reduces with increasing the size of the lip. From this parametric study, it is observed that the lip size of the section has a significant effect on the strength and behaviour of the column section. For the particular selected cross section, the maximum lip size is limited to 50 mm to minimize torsional rigidity and local buckling of lips.

### Effect of Variation of Flange Width

Figure 8d demonstrates the relationship between the flange width (E3) and the ultimate load of the column for different lengths and flange width varied from 30 to 100 mm with increment of 10 mm while keeping all other factors same of mean cross section geometries for each finite element analysis. For the particular length, load carrying capacity of the column increases with the increase in the flange width and is reduced by the increasing flange width. Because of the increase in the flange width, the local buckling occurs at the flange. From this parametric study, it is observed that the flange width of the section has a significant effect on the load carrying capacity of the column.

### Effect of Variation of Depth of Section

The effect of variation of the depth of the section is demonstrated in Fig. 8e for three lengths (500, 1000 and 2000 mm) and depth of the sections varied from 30 to 80 mm with the basic value of the section dimensions as defined in Table 3. It is observed that the depth of the member has a significant effect on the ultimate strength and behaviour of the columns. From the Fig. 8e, it can be observed that, the resistance of the column increases with

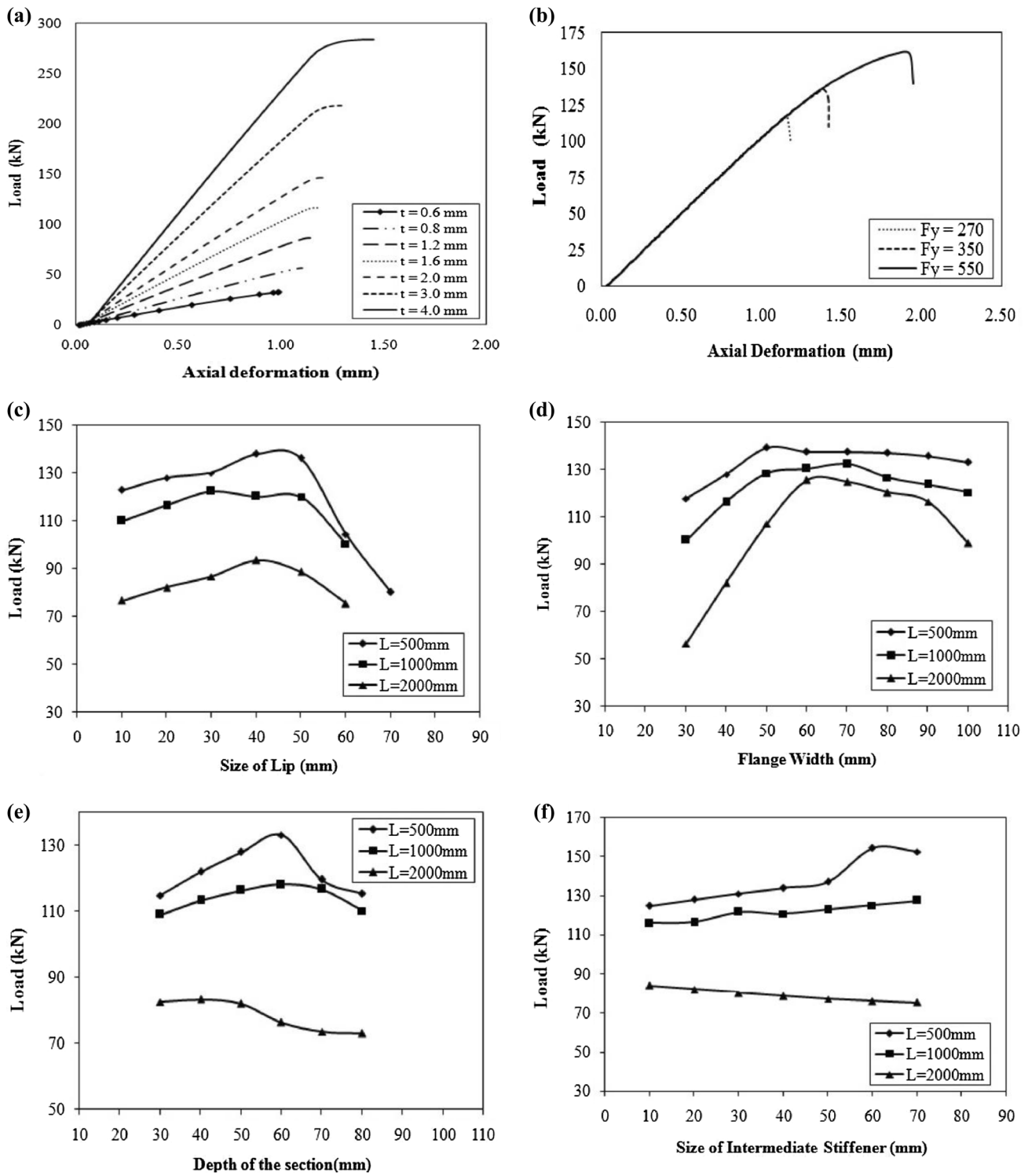


**Fig. 8** Effect of variation: **a** Thickness. **b** Yield stress. **c** Size of lip. **d** Flange width. **e** Depth of the section. **f** Size of intermediate stiffener

the increase in the depth of the section and is reduced by the increasing depth of the section. Because of the increase in the depth of the section, the local buckling occurs on the web.

### Effect of Variation of Size of Intermediate Stiffener

In this parametric study, size of intermediate stiffener varied from 10 to 70 mm with three different lengths (500, 1000 and 2000 mm) and all other parameters is constant.

**Table 4** Effect yield stress and thickness variation

Effect of Yield stress variation			Effect of thickness variation			
Thickness (mm)	Yield stress (N/mm <sup>2</sup> )	Load (kN)	Yield stress (N/mm <sup>2</sup> )	Thickness (mm)	Load (kN)	
0.60	270	32.62	270	0.60	32.62	
	350	32.62		0.80	56.71	
	550	32.62		1.20	86.48	
0.80	270	56.71	270	1.60	116.16	
	350	62.51		2.00	145.94	
	550	65.51		3.00	217.61	
1.20	270	86.48	270	4.00	283.59	
	350	98.83		350	0.60	32.62
	550	112.84			0.80	62.51
1.60	270	116.16	270	1.20	98.83	
	350	135.74		1.60	135.74	
	550	160.60		2.00	173.79	
2.00	270	145.94	270	3.00	265.58	
	350	173.79		4.00	348.03	
	550	211.54		550	0.60	32.62
3.00	270	217.61	0.80		65.51	
	350	265.58	1.20	112.84		
	550	344.01	1.60	160.60		
4.00	270	283.59	270	2.00	211.54	
	350	348.03		3.00	344.01	
	550	466.40		4.00	466.40	

The effect of variation of size of intermediate stiffener is demonstrated in Fig. 8f. From the Fig. 8f, it can be observed that for short and intermediate column the ultimate load increases with the increase in the size of intermediate stiffener. But for the long column, load carrying capacity of the column decreases with an increase in the size of intermediate stiffener (W/t).

### Theoretical Investigation

The nominal unfactored design strengths  $P_{DSM}$  (least of local, distortional and flexural buckling) calculated using the direct strength method in Eqs. (1)–(4) are compared with the FEA strengths ( $P_{ANSYS}$ ). The DSM -to-FEA strength is ( $P_{DSM}/P_{ANSYS}$ ) shown in Table 6.

$$P_n = \text{Min}(P_{ne}, P_{nl}, P_{nd}) \tag{1}$$

$$P_{ne} = \begin{cases} (0.658)^{\lambda_c^2} P_y & \text{for } \lambda_c \leq 1.5 \\ \left(\frac{0.877}{\lambda_c^2}\right) P_y & \text{for } \lambda_c > 1.5 \end{cases} \tag{2}$$

where  $\lambda_c = \sqrt{P_y/P_{cre}}$  and  $P_y = Af_y$ .  $P_y$  is the squash load; A is the gross cross-sectional area;  $f_y$  is the yield stress and  $P_{cre}$  is the critical elastic column buckling load in flexural

buckling/flexural–torsional/torsional. The nominal axial strength ( $P_{nl}$ ) for local buckling is

$$P_{nl} = \begin{cases} P_{ne} & \text{for } \lambda_1 \leq 0.776 \\ \left(1 - 0.15 \left(\frac{P_{cr1}}{P_{ne}}\right)^{0.4}\right) \left(\frac{P_{cr1}}{P_{ne}}\right) P_{ne} & \text{for } \lambda_1 > 0.776 \end{cases} \tag{3}$$

where  $\lambda_1 = \sqrt{P_{ne}/P_{cr1}}$ ,  $P_{cr1}$  is the critical elastic local column buckling load and  $P_{ne}$  is defined in Eq. (2). The nominal axial strength ( $P_{nd}$ ) for distortional buckling is

$$P_{nd} = \begin{cases} P_y & \text{for } \lambda_d \leq 0.561 \\ \left(1 - 0.25 \left(\frac{P_{crd}}{P_y}\right)^{0.6}\right) \left(\frac{P_{crd}}{P_y}\right)^{0.6} P_y & \text{for } \lambda_d > 0.561 \end{cases} \tag{4}$$

where  $\lambda_d = \sqrt{P_y/P_{crd}}$  and  $P_{crd}$  is the critical elastic distortional column buckling load.

The mean and standard deviation of  $P_{DSM}/P_{ANSYS}$  are 0.96 and 0.19 respectively. From this it is observed that the Direct Strength method specification is under estimate for the strength of new inventive stiffened CFS section, i.e. the ratio of  $P_{DSM}/P_{ANSYS}$  is less than one. Since, the design equation has underestimated the column strength, hence a

**Table 5** Comparison of FEA and DSM results

Specimen ID	Ultimate load (kN)		$\frac{P_{DSM}}{P_{ANSYS}}$	Specimen ID	Ultimate load (kN)		$\frac{P_{DSM}}{P_{ANSYS}}$
	$P_{ANSYS}$	$P_{DSM}$			$P_{ANSYS}$	$P_{DSM}$	
SC-E1-10	122.60	112.2	0.92	LC-E3-90	116.23	131.73	1.13
SC-E1-15	127.77	120.44	0.94	LC-E3-100	98.56	131.14	1.33
SC-E1-20	130.07	127.77	0.98	SC-E5-30	114.63	113.43	0.99
SC-E1-30	137.71	140.78	1.02	SC-E5-40	121.81	117.33	0.96
SC-E1-40	136.04	136.06	1.00	SC-E5-50	127.77	120.44	0.94
SC-E1-50	104.25	125.24	1.20	SC-E5-60	133.01	122.66	0.92
SC-E1-60	80.05	117.65	1.47	SC-E5-70	119.40	124.08	1.04
IC-E1-10	109.87	96.38	0.88	SC-E5-80	115.23	124.87	1.08
IC-E1-15	116.15	98.49	0.85	IC-E5-30	108.75	100.12	0.92
IC-E1-20	122.09	101.05	0.83	IC-E5-40	113.09	99.59	0.88
IC-E1-30	119.92	106.78	0.89	IC-E5-50	116.15	98.49	0.85
IC-E1-40	119.73	116.16	0.97	IC-E5-60	117.89	97.00	0.82
IC-E1-50	100.25	119.93	1.20	IC-E5-70	116.53	95.34	0.82
IC-E1-60	76.27	113.74	1.49	IC-E5-80	110.00	93.66	0.85
LC-E1-10	76.36	55.75	0.73	LC-E5-30	82.32	57.91	0.70
LC-E1-15	81.92	65.52	0.80	LC-E5-40	83.17	61.71	0.74
LC-E1-20	86.43	73.46	0.85	LC-E5-50	81.92	65.52	0.80
LC-E1-30	93.36	91.89	0.98	LC-E5-60	76.11	69.32	0.95
LC-E1-40	88.42	102.71	1.88	LC-E5-70	73.32	71.93	0.94
LC-E1-50	75.30	107.91	1.22	LC-E5-80	72.85	75.68	1.04
LC-E160	54.57	99.46	1.32	SC-E7-10	124.69	76.62	0.61
SC-E3-30	117.52	109.56	0.93	SC-E7-20	127.77	120.44	0.94
SC-E3-40	127.77	120.44	0.94	SC-E7-30	130.75	124.25	0.95
SC-E3-50	139.03	130.37	0.94	SC-E7-40	133.80	127.71	0.95
SC-E3-60	137.39	139.64	1.02	SC-E7-50	136.89	130.88	0.96
SC-E3-70	137.24	147.78	1.08	SC-E7-60	154.21	133.8	0.87
SC-E3-80	136.85	154.88	1.13	SC-E7-70	152.31	136.52	0.90
SC-E3-90	135.52	182.24	1.34	IC-E7-10	115.68	99.06	0.86
SC-E3-100	132.84	165.93	1.25	IC-E7-20	116.15	98.49	0.85
IC-E3-30	99.92	90.70	0.91	IC-E7-30	121.40	98.09	0.81
IC-E3-40	116.15	98.49	0.85	IC-E7-40	120.57	100.85	0.84
IC-E3-50	128.21	110.49	0.86	IC-E7-50	122.62	97.66	0.80
IC-E3-60	130.10	109.49	0.84	IC-E7-60	124.85	97.57	0.78
IC-E3-70	132.13	113.61	0.86	IC-E7-70	127.34	97.52	0.77
IC-E3-80	126.42	117.16	0.93	LC-E7-10	83.80	62.59	0.75
IC-E3-90	123.56	120.34	0.97	LC-E7-20	81.92	65.52	0.80
IC-E3-100	120.24	123.26	1.03	LC-E7-30	80.20	67.42	0.84
LC-E3-30	56.33	47.95	0.85	LC-E7-40	78.58	69.32	0.88
LC-E3-40	81.92	65.52	0.80	LC-E7-50	77.17	71.22	0.92
LC-E3-50	106.87	80.14	0.75	LC-E7-60	75.93	74.28	0.98
LC-E3-60	125.31	123.08	0.98	LC-E7-70	75.17	76.21	1.01
LC-E3-70	124.58	108.05	0.87	Mean			0.96
LC-E3-80	120.09	120.19	1.00	Standard deviation			0.19

modification factor in the DSM equations are suggested to evaluate the new inventive stiffened CFS section. The comparison of  $P_{DSM}/P_{ANSYS}$  is pictured in Fig. 9. Hence, a

regression analysis is performed for the results of 126 FEA. From the regression analysis, it is suggested that a modification factor of 1.029 is to recommend to the ultimate

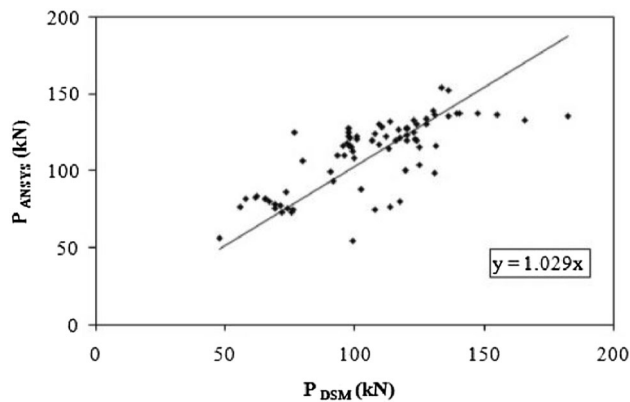


**Fig. 9** Comparison of  $P_{ANSYS}$  and  $P_{DSM}$

**Table 6** Verification of design equation [14]

Specimen ID as per literature	Ultimate load (kN)			$\frac{P_{Design}}{P_{EXP}}$
	$P_{EXP}$	$P_{DSM}$	$P_{Design}$	
2B	243.00	245.45	252.57	1.04
3B	347.00	347.00	357.06	1.03
4A	344.00	344.00	353.98	1.03
4B	342.00	335.29	345.02	1.01
Mean				1.03
Standard deviation				0.01

strength of new inventive stiffened CFS column section estimated by the Direct Strength method.

The accuracy of the proposed design modification is verified by comparing its results to selected available experimental results from past literature of (Chen et al. [14]) and results are presented in Table 6. The mean and standard deviation of  $P_{Design}/P_{EXP}$  is 1.03 and 0.01 respectively. It shows that the proposed design alteration provides the superlative results compared to the Direct Strength method.

## Summary and Conclusions

This study deals with the theoretical and numerical investigation on the ultimate strength and behaviour of pinned end new inventive stiffened CFS section. Numerical investigation is performed by means of the commercial software ANSYS. The numerical model, including the material and geometric imperfections, has been calibrated against the test results obtainable from the literature. Theoretical analyses are carried out by using the Direct Strength Method of specifications for cold formed steel structures. Buckling plot is plotted using linear elastic buckling analysis software (CUFSM). A total of 126

systematic parametric studies is performed using the confirmed FEM. The conclusions of the study are summarized as follows:

- FEA predictions provide the good agreement with the test results.
- Stiffened element at the flanges increases the torsional rigidity of the unstiffened element and intermediate stiffener on the web performed well against local buckling.
- Thickness and yield stress significantly affect the strength and behaviour of the column. Similarly, lip size and depth of the section, size of intermediate stiffener adversely affects the strength of a long column.
- The existing DSM underestimates the ultimate loads of new inventive stiffened CFS section and therefore modification factor is proposed for the proposed section. The modification factors provide better results to the experimental results.

## References

1. T.P. Desmond, T. Pekoz, G. Winter, Edge stiffeners for thin-walled members. *J. Struct. Eng.* **107**(2), 329–353 (1981)
2. Y.B. Kwon, G.J. Hancock, Test of cold-formed channels with local and distortional buckling. *J. Struct. Eng.* **117**(7), 1786–1803 (1992). [https://doi.org/10.1061/\(ASCE\)0733-9445](https://doi.org/10.1061/(ASCE)0733-9445)
3. J. Yan, B. Young, Column tests of cold-formed steel channels with complex stiffeners. *J. Struct. Eng.* **128**(6), 737–745 (2002). [https://doi.org/10.1061/\(ASCE\)0733-9445](https://doi.org/10.1061/(ASCE)0733-9445)
4. D. Yang, G.J. Hancock, Compression tests of high strength steel channel columns with interaction between local and distortional buckling. *J. Struct. Eng.* **130**(12), 1954–1963 (2004). [https://doi.org/10.1061/\(ASCE\)0733-9445](https://doi.org/10.1061/(ASCE)0733-9445)
5. N. Silvestre, D. Camotim, P.B. Dinis, Post-buckling behaviour and direct strength design of lipped channel columns experiencing local/distortional interaction. *J. Constr. Steel Res.* **73**, 12–30 (2012). <https://doi.org/10.1016/j.jcsr.2012.01.005>
6. B.W. Schafer, Local, distortional, and euler buckling of thin-walled columns. *J. Struct. Eng.* **128**(3), 289–299 (2002). [https://doi.org/10.1061/\(ASCE\)0733-9445](https://doi.org/10.1061/(ASCE)0733-9445)
7. Y.B. Kwon, B.S. Kim, G.J. Hancock, Compression tests of high strength cold-formed steel channels with buckling interaction. *J. Constr. Steel Res.* **65**, 278–289 (2009). <https://doi.org/10.1016/j.jcsr.2008.07.005>
8. P.B. Dinis, D. Camotim, E.M. Batista, E. Santos, Local/distortional/global mode coupling in fixed lipped channel columns: behaviour and strength. *Adv. Steel Constr.* **7**(1), 113–130 (2011)
9. P.B. Dinis, E.M. Batista, D. Camotim, E. Santos, Local–distortional–global interaction in lipped channel columns: experimental results, numerical simulations and design considerations. *Thin Walled Struct.* **61**, 2–13 (2012). <https://doi.org/10.1016/j.tws.2012.04.012>
10. P. Manikandan, N. Arun, Numerical investigation on cold-formed steel lipped channel columns with intermediate web stiffeners. *J. Inst. Eng. (India) Series A.* **97**(1), 1–7 (2016). <https://doi.org/10.1007/s40030-016-0148-0>

11. M.V. Anil Kumar, V. Kalyanaraman, Distortional buckling of CFS stiffened lipped channel compression members. *J. Struct. Eng.* (2014). [https://doi.org/10.1061/\(ASCE\)ST.1943-541X.0001027.140\(12\)](https://doi.org/10.1061/(ASCE)ST.1943-541X.0001027.140(12))
12. P.B. Dinis, B. Young, D. Camotim, Strength, interactive failure and design of web-stiffened lipped channel columns exhibiting distortional buckling. *Thin Walled Struct.* **81**, 195–209 (2014). <https://doi.org/10.1016/j.tws.2013.09.016>
13. L. Li, J. Chen, An analytical model for analysing distortional buckling of cold-formed steel sections. *Thin Walled Struct.* **46**, 1430–1436 (2008). <https://doi.org/10.1016/j.tws.2008.03.005>
14. J. Chen, Y. He, W.L. Jin, Stub column tests of thin-walled complex section with intermediate stiffeners. *Thin-Walled Struct.* **48**, 423–429 (2010). <https://doi.org/10.1016/j.tws.2010.01.008>
15. S. Huang, J. Chen, W. Jin, Numerical investigation and design of thin-walled complex section steel columns. *J. Zhejiang Univ. Sci. A. (Appl. Phys. Eng.)* **12**(2), 131–135 (2011)
16. M. Seif, B. Schafer, Design of locally slender structural steel columns. *J. Struct. Eng.* **140**, 1–10 (2014). [https://doi.org/10.1061/\(ASCE\)ST.1943-541X.0000889](https://doi.org/10.1061/(ASCE)ST.1943-541X.0000889)
17. H. Teter, S. Debski, Samborski, On buckling collapse and failure analysis of thin-walled composite lipped-channel columns subjected to uniaxial compression. *Thin Walled Struct.* **85**, 324–331 (2014). <https://doi.org/10.1016/j.tws.2014.09.010>
18. A. Landesmann, D. Camotim, On the Direct Strength Method (DSM) design of cold-formed steel columns against distortional failure. *Thin Walled Struct.* **67**, 168–187 (2013). <https://doi.org/10.1016/j.tws.2013.01.016>
19. M. Casafont, M.M. Pastor, F. Roure, J. Bonada, T. Peköz, Design of steel storage rack columns via the direct strength method. *J. Struct. Eng.* **139**(5), 669–679 (2013). [https://doi.org/10.1061/\(ASCE\)ST.1943-541X.0000620](https://doi.org/10.1061/(ASCE)ST.1943-541X.0000620)
20. Z. He, X. Zhou, Z. Liu, M. Chen, Post-buckling behaviour and DSM design of web-stiffened lipped channel columns with distortional and local mode interaction. *Thin Walled Struct.* **84**, 189–203 (2014). <https://doi.org/10.1016/j.tws.2014.07.001>
21. N. Silvestre, D. Camotim, P.B. Dinis, Direct strength prediction of lipped channel columns experiencing local-plate/distortional interaction. *Adv. Steel Constr.* **5**(1), 49–71 (2009)
22. Y. Zhang, C. Wang, Z. Zhang, Tests and finite element analysis of pin-ended channel columns with inclined simple edge stiffeners. *J. Constr. Steel Res.* **63**, 383–395 (2007). <https://doi.org/10.1016/j.jcsr.2006.04.008>
23. B.W. Schafer, T. Pekoz, Computational modeling of cold-formed steel characterizing geometric imperfections and residual stresses. *J. Constr. Steel Res.* **47**, 193–210 (1998). [https://doi.org/10.1016/S0143-974X\(98\)00007-8](https://doi.org/10.1016/S0143-974X(98)00007-8)
24. B.W. Schafer, Z. Li, C.D. Moen, Computational modeling of cold-formed steel. *Thin Walled Struct.* **48**, 752–762 (2010). <https://doi.org/10.1016/j.tws.2010.04.008>